30 minutes, pure hybridization buffer is reintroduced to the sensors. A mean net resonance wavelength shift of 74 pm after 30 minutes is observed in 8 microring sensors simultaneously. This wavelength shift is comparable

to values reported in literature [6]. This proves both the ability of our sensors to detect complementary DNA sequences and the possibility of a multiplexed detection assay.

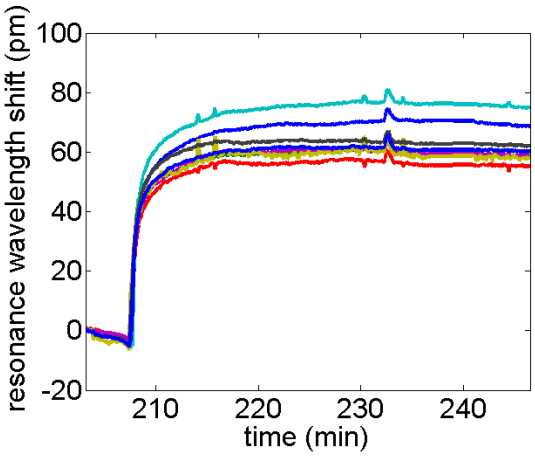

Figure 1. Binding curve for 10nM complementary DNA sequence solution.

3. BINDING CURVE CORRUPTION

Since the resonance splitting in our microring sensors can easily amount to a measurable erroneous, unexpected resonance splitting can severely compromise a recorded binding curve. As resonance splitting is partly a consequence of random process variations on the waveguide edges, it is impossible to predict its strength. This means a resonance selection algorithm cannot differentiate split and unsplit resonances. Jumps between both modes of a split resonance can lead to false positive or even false negative results when the sensor is implemented in a lab-on-a-chip setting.

4. ORIGIN OF RESONANCE SPLITTING

A perfectly symmetric microring resonator mode is twofold degenerate. Both clockwise (CW) and counter-clockwise (CCW) propagation are possible in the microring and both modes are uncoupled. This degeneracy is lifted when the CW-mode and CCW-mode become coupled. Surface roughness on the waveguide edges and the proximity of bus waveguides for microring interrogation form deviations from circular symmetry. These deviations cause forward propagating light to scatter back into the opposite direction, exciting a CCW-mode from a CW-mode and vice versa. Standing-wave modes as a symmetric and antisymmetric superposition of the traveling waves can be considered as the new eigenmodes of the system. They will however no longer be degenerate as a consequence of the symmetry breaking coupling [7]. If the linewidth of the resonance is small enough to distinguish both modes, the resonance splitting will be visible in the output signal. This occurs for high quality resonances. Evidence of this effect is provided in figure 2, which shows both the pass-port and add-port spectrum of a microring in add-drop configuration. Only the input port is excited, so ideally, no power is present in the CCW-mode and the add-port remains dark. The measurement shows that backscattering in the microring waveguide cannot be neglected, resulting in significant power in the add-port and resonance-splitting in the pass-signal amounting up to 50 pm.

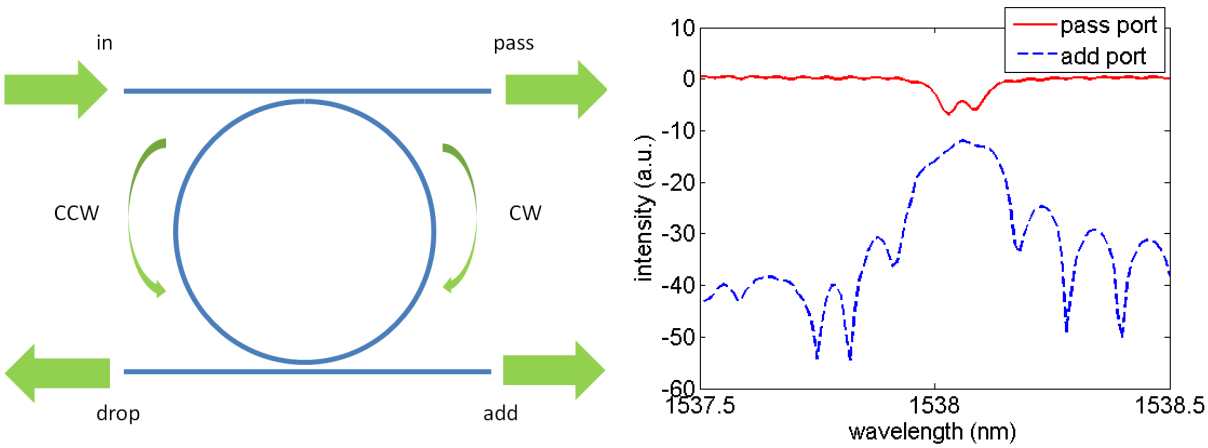

Figure 2. Microring in add-drop configuration (left). Measured spectra showing resonance splitting and backscattered power (right).

5. INTEGRATED INTERFEROMETRIC CIRCUIT

As demonstrated in [8], an interferometric approach can be used to access the normal modes of the microring resonator in an output signal. We have implemented this in an integrated circuit on a single SOI-chip. A layout of the circuit is provided in Fig. 3.

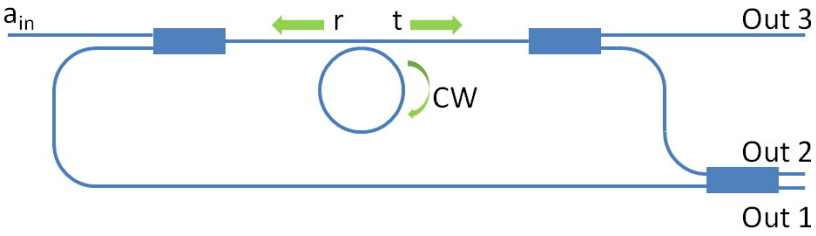

Figure 3. Layout of the integrated interferometric circuit.

Vertical grating couplers are used to couple light from a tunable laser light source into the circuit and collect the power at the output. The input light excites a CW-mode in the microring resonator, a CCW-mode is excited as a consequence of mode-coupling. The normal modes of the microring are a symmetric and antisymmetric superposition of the CW and CCW-mode, so we can express them as follows:

$$a\pm = \frac{1}{\sqrt{2}}\left(a_{CW} \pm a_{CCW}\right) \tag{1}$$

If the coupling per unit time between the bus waveguide and the microring is represented by κ, the fields transmitted and reflected by the resonator are

$$t = \frac{1}{\sqrt{2}} a_{in} + \kappa a_{CW}, r = \kappa a_{CCW} \tag{2}$$

Both fields are combined in a multimode interferometer (MMI), which results in the following signals at the different output ports. φ denotes the phase difference between the combining waves.

$$\begin{aligned} out_1 &= \frac{1}{2}\left(\frac{1}{\sqrt{2}} a_{in} + \kappa a_{CW} + \mathrm{e}^{i\phi} a_{CCW}\right) \\ out_2 &= \frac{1}{2}\left(\frac{1}{\sqrt{2}} a_{in} + \kappa a_{CW} - \mathrm{e}^{i\phi} a_{CCW}\right) \\ out_3 &= \frac{1}{\sqrt{2}} t \end{aligned} \tag{3}$$

If we design the circuit such that the phase difference between the reflected and transmitted wave equals a multiple of 0 or π, we see that the signals in output one and two are proportional to the normal modes of the resonator. At the same time, output three is proportional to the pass-signal of the microring resonator in the all-pass configuration. This means we have access to the unsplit, high-Q normal modes of the cavity. If the detection limit of a biosensor is limited by the quality-factor of the resonance, this provides a tool to improve the detection limit significantly. Higher resonator Q-factors give rise to lower detection limits.

6. EXPERIMENTAL RESULTS

The circuit from Fig. 3 is designed and processed in a CMOS pilot line at imec. Using the vertical in- and output couplers on the waveguides, the chip can easily be measured in a fiber-to-fiber configuration. For the junction regions where waveguides are combined and split, MMI 2 × 1 and MMI 2 × 2 couplers are used. The coupling from the microring to the waveguide is ensured by weak evanescent coupling to a neighbouring bus waveguide. To obtain the measured spectra, a SANTEC TSL-510 tunable laser source is used to generate the input signals. Output intensities are measured by a HP-8153 optical power meter. The laser wavelength is swept in 10 pm steps during recording of the power. Figure 4 shows the recorded spectra at the three outputs of the circuit. Output one and two are proportional to the normal modes of the resonator, output three returns the all-pass spectrum. We clearly see the all-pass spectrum shows severe splitting of 60 pm in the resonance. This values is comparable to the 3 dB-bandwidth of the normal mode in output one. The Q-factors of the recorded resonances in output one amount to 2.2×10^4, which is almost a twofold improvement of the resonance quality from output three (1.28×10^4). Notice the distinct asymmetrical shape of the resonance in output two which makes unambiguous definition of a Q-value difficult. Additionally, the extracted normal modes do not correspond exactly with the

normal modes we can distinguish in the all-pass signal. This non-ideal behaviour is a consequence of fabrication variations. The 2 × 2 MMI is especially sensitive to this and is not exactly balanced as a result. Also the phase relation between the reflected and the transmitted wave differs slightly from the required value of $k\pi$. This can be solved by careful tuning of the waveguide structures.

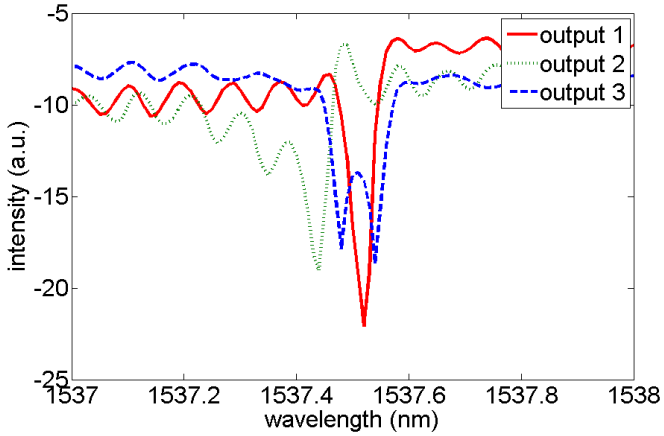

Figure 4. Measured output spectra of the circuit. Output one clearly shows the improvement of the resonance shape compared to the all pass signal in output three.

7. CONCLUSIONS

In this paper, we have demonstrated the successful recognition of a complementary DNA sequence. We have also discussed the problem of microring resonance splitting and shown the possibility of in integrated interferometric setup to resolve this on the SOI-platform. The access to the unsplit normal modes of the resonator allows the improvement of the detection limit of microring resonator biosensors.

ACKNOWLEDGEMENTS

The author would like to acknowledge the 'Bijzonder Onderzoeksfonds' (BOF) for a research grand. Part of this work was performed in the framework of the RAPP-ID project which provided fruitful collaborations. RAPP-ID was supported by the Innovative Medicines Initiative, a public-private partnership between the European Union, and the European Federation of Pharmaceutical Industries and Associations (RAPP-ID project, grant agreement, no. 115153).

REFERENCES

[1] K. De Vos, J. Girones, T. Claes, Y. De Koninck, S. Popelka, E. Schacht, R. Baets, and P. Bienstman, "Multiplexed antibody detection with an array of silicon-on-insulator microring resonators," *IEEE Photonics Journal*, vol. 1, no. 4, pp. 225–235, Oct. 2009.

[2] C. L. Arce, K. D. Vos, T. Claes, K. Komorowska, D. V. Thourhout, and P. Bienstman, "Silicon-on-insulator microring resonator sensor integrated on an optical fiber facet," *IEEE Photonics Technology Letters*, vol. 23, no. 13, pp. 890–892, 2011.

[3] T. Claes, W. Bogaerts, and P. Bienstman, "Experimental characterization of a silicon photonic biosensor consisting of two cascaded ring resonators based on the Vernier-effect and introduction of a curve fitting method for an improved detection limit," *Optics Express*, vol. 18, no. 22, pp. 22 747–22 761, 2010.

[4] W. Bogaerts, P. D. Heyn, T. V. Vaerenbergh, K. D. Vos, S. Kumar, T. Claes, P. Dumon, P. Bienstman, D. V. Thourhout, and R. Baets, "Silicon microring resonators," *Laser & Photonics Reviews*, vol. 6, no. 1, pp. 47–73, 2011.

[5] T. Claes, J. Molera, K. De Vos, E. Schacht, R. Baets, and P. Bienstman, "Label-free biosensing with a slot-waveguide-based ring resonator in silicon on insulator," *IEEE Photonics Journal*, vol. 1, no. 3, pp. 197–204, Sep. 2009.

[6] A. J. Qavi, R.C. Bailey, "Multiplexed detection and label-free quantitation of microRNAs using arrays of silicon photonic microring resonators", *Angewandte Chemie International Edition*, vol. 49, pp. 4608–4611, Jun. 2010.

[7] T. J. Kippenberg, S. M. Spillane, and K. J. Vahala, "Modal coupling in traveling-wave resonators," *Optics letters*, vol. 27, no. 19, pp. 1669–71, Oct. 2002.

[8] J. Knittel, T. G. McRae, K. H. Lee, and W. P. Bowen, "Interferometric detection of mode splitting for whispering gallery mode biosensors," *Applied Physics Letters*, vol. 97, no. 12, p. 123704, 2010.